

Applicability of the inverse dispersion method to measure emissions from animal housings

Marcel Bühler^{1,2}, Christoph Häni¹, Albrecht Neftel³, Patrice Bühler¹, Christof Ammann⁴, Thomas Kupper¹

- 5 ¹School of Agricultural, Forest and Food Sciences HAFL, Bern University of Applied Sciences, Zollikofen, 3052, Switzerland
²Department of Biological and Chemical Engineering, Aarhus University, Aarhus, 8000, Denmark
³Nefel Research Expertise, Wohlen bei Bern, 3033, Switzerland
⁴Climate and Agriculture Group, Agroscope, Zürich, 8046, Switzerland

Correspondence to: Marcel Bühler (mb@bce.au.dk)

Formatted: German (Switzerland)

- 10 **Abstract.** Emissions from agricultural sources substantially contribute to global warming. The inverse dispersion method (IDM) has been successfully used for emission measurement from various agricultural sources. The ~~method-IDM~~ has also been validated in multiple studies with artificial gas releases mostly ~~on-in~~ open fields. Release experiments from buildings have been ~~very rarely conducted~~ and were partly affected by additional nearby sources of the ~~same-target~~ gas. ~~What is also lacking are s~~Specific release studies for naturally ventilated animal housings ~~are lacking~~. In this study, a known and predefined amount of methane was released from an artificial source inside a barn that ~~mimicked~~s a naturally ventilated dairy housing and IDM recovery rates, using a backward Lagrangian stochastic model, were determined. For concentration measurements, open-path devices (OP) with a path length of 110 m were placed in downwind direction of the barn at ~~a distance of~~ ~~distances of~~ 50 m, 100 m, 150 m, and 200 m (h equals the height of the highest obstacle) and ~~and additionally,~~ a 3D ultrasonic anemometer (UA) ~~was placed~~ ~~was placed~~ in the middle of the ~~first three~~ OP paths at 50 m, 100 m and 150 m.
- 15 Upwind of the barn, an additional OP and an UA were installed. The median IDM recovery rates ~~of the experiment depending on the used OP and~~ determined with the UA placed upwind of the barn and the downwind OP combination ranged between 0.565 - 0.745. It is concluded that for the present study case, the effect of the building and a tree in the main wind axis led to a systematic underestimation of the ~~inverse dispersion method~~ IDM derived emission rate probably due to deviations of the wind field and turbulent dispersion from the ~~ideal underlying~~ assumptions ~~of the used dispersion model~~.

Formatted: Not Highlight

Formatted: Not Highlight

25 1 Introduction

- ~~The growth in atmospheric methane (CH₄) concentration is largely due to emissions from the fossil fuels, the agriculture, and the waste sectors (Arias et al., 2021). For the period 2008-2017, global MCH₄ methane (CH₄) emissions from agriculture and waste management contributed 56% of the total anthropogenic CH₄ emissions (Saunio et al., 2020), is the second most important greenhouse gas after carbon dioxide. In the last decade, atmospheric CH₄ concentrations were dominated by emissions from fossil fuels, agriculture, landfills, and the waste management sector (Stocker et al., 2013). Within the livestock~~

Formatted: Subscript

Formatted: Font: 6 pt

35 livestock sector at a global scale, CH₄ mainly originates from enteric fermentation in the digestive tract of ruminants and to a minor extent from emissions from manure management (Gerber et al., 2013). ~~(Gerber et al., 2013; Gerber, 2013)(Gerber, 2013)~~. A common housing system for cattle is loose housing in naturally ventilated buildings. ~~(Sommer et al., 2013)(Sommer et al., 2013)~~. To improve national emission inventories and test mitigation effects under real-world conditions, accurate measurements are necessary. For confined sources of greater complexity, the inverse dispersion method (IDM) has ~~been become established in the recent years. The IDM is a micrometeorological method that combines the concentration measurements of the up-concentration enhancement and~~ downwind of the spatially defined source with an atmospheric dispersion model. For agricultural emissions, most often ~~the~~ backward Lagrangian stochastic (bLS) model ~~approach by~~ Flesch et al. (1995) is used. ~~This IDM with a~~ bLS model has been verified in multiple release experiments on open fields that reflect ideal conditions in terms of Monin-Obukhov-Similarity theory. ~~(Flesch et al., 2004) (Flesch et al., 2004)~~. Ideal conditions for the bLS model are a horizontally homogeneous surface layer and a distance between source and sensors of less than 1 km (Flesch et al., 1995). ~~Also, under less ideal conditions in terms of Monin-Obukhov-Similarity theory, the IDM-bLS model showed its aptitude for a wide range of sources (e.g., Bühler et al., 2022; Bühler et al., 2021; Flesch et al., 2009; Laubach et al., 2013; Vanderzaag et al., 2014) (e.g., Bühler et al., 2022; Bühler et al., 2021; Flesch et al., 2009; Flesch et al., 2013; Laubach et al., 2013; Vanderzaag et al., 2008)~~. However, there are only few studies available, where the gas was released within or close to a building ~~or~~ structure. Baldé et al. (2016) ~~Baldé et al. (2016a,b)~~ and Hrad et al. (2021) ~~Hrad et al. (2021)~~ released CH₄ at real-world facilities in addition to the CH₄ from sources existing at the sites. ~~McGinn et al. (2006) McGinn et al. (2006) McGinn et al. (2006) (McGinn et al., 2006)~~ conducted a release experiment at a barn with three release positions on top of the roof and three positions outside the walls of the barn. Gao et al. (2010) ~~Gao et al. (2010)~~ released CH₄ via four side vents of a barn. The barn in the study of Gao et al. (2010) ~~Gao et al. (2010)~~ is comparable to a mechanically ventilated building which is common for fattening pigs or poultry.

In this ~~paper study~~, we present an experiment with artificial release of CH₄ within a building similar to a naturally ventilated dairy housing. The goal of this experiment was to test ~~the IDM with the IDM-bLS modelling for the quantification of for~~ emissions ~~measurements~~ from an agricultural building with natural ventilation under as realistic conditions as possible. ~~to optimise the quality of the measurement results and minimise the uncertainty range of the IDM.~~ Compared to ~~Gao et al. (2010) Gao et al. (2010)~~, multiple 3D ultrasonic anemometers were available in our experiment. Thus, the focus was on the positioning of the open-path concentration sensors and the ultrasonic anemometers at different horizontal distances downwind of the source.

2 Material and Methodology

2.1 Experimental site and periods

The release experiment was conducted in a barn located in the Central Plateau of Switzerland (47.04307 N, 7.22691 E). The barn allowed a setup which mimicked a naturally ventilated dairy housing. About 350 m northeast of the barn ~~was~~ a river with

Formatted: Not Highlight

Formatted: Font color: Background 1

Formatted: Not Highlight

Formatted: Font: 6 pt

dams on each side that are 4 m higher dams on each side and about than the agricultural land surrounding the barn. 25 m high trees on it. There were no other obstacles between the barn and the dam. The canopy height directly around the barn was 20 cm or and lower and remained constant over the course of the measurements. The barn is was 25 m long, 17 m wide and 7 m high (Fig. 1 Fig. 1). During the release experiment, about 17% of the barn's surface was occupied by storage boxes stacking up almost to the ceiling. Despite other agricultural equipment inside the barn, about 33% of the south end of the barn were empty. The barn had on each transverse side a 4.8 m wide and 4.0 m high gate. During the CH₄ releases, the gate on the south side was fully open, whereas the gate on the north side was opened 1.3 m. The north facing wall of the barn was impermeable, however the south wall and the longitudinal side walls exhibited small holes and cracks all over the wall allowing for air exchange through the wall. At both longitudinal sides of the barn there were gaps of about 0.6 m below the roof which were covered by cracked plastic sheets. About 20 m southwest of the barn was a tree of about 15 m height (Fig. 1 Fig. 1).



Fig. 1. Barn used for the CH₄ release experiment and the adjacent tree. In the background a river dam with trees on it is visible. The photo was taken from the southwest side of the barn. In the foreground is a 3D ultrasonic anemometer (UA-50m-2.0h).

A petrol-powered generator (Honda EU 20i), located outside the barn at the southeast side, provided the necessary power for all the instruments.

The wind and concentration measurements lasted over several weeks from 05 March to 26 March 2021. A first intercomparison (IC1) of the open-path devices was conducted from 05 March to 10 March 2021. The measurement campaign (MC) took place from 18 March 2021 11:00 to 21 March 2021 13:00 UTC+1. Within this MC, CH₄ was released with a CH₄ source inside the barn from 19 March 2021 10:30 to 19 March 2021 16:40 UTC+1, denoted as daytime release - and 19 March 2021 21:50 to 20 March 2021 06:50 UTC+1, denoted as nighttime release. The second intercomparison (IC2) of the open-path devices was

conducted from 21 March 2021 15:00 to 26 March 2021 10:00 UTC+1. CH₄ was also released during part of IC2 ([supporting information, SI-1](#)).

85 2.2 Methane source

For the release during MC and half of IC2, a gas bundle of 12 cylinders with 50 L at 200 bars, each with high-purity (> 99.5%_{mol}) CH₄, was used to supply the CH₄ source. For the rest of the release in IC2, one gas cylinder with 50 L at 200 bars was used. Attached to the bundle was a pressure regulator ([Fig. 2Fig-2](#)). The pressure on the high-pressure side was measured with a digital pressure sensor (LEX1-Ei / 200bar / 81770.5, Keller AG, Winterthur, Switzerland). The low-pressure side was set to 3 bars. The pressure regulator and the mass flow controller (MFC, EL-FLOW Select F-202AV-M20-AGD-22-V, Bronkhorst High-Tech B.V., Ruurlo, The Netherlands) were connected by a polyethylene naphthalate (PEN) tubing (FESTO, PEN-16X2,5-BL-100 551449) with an inner diameter of 10.8 mm. After the MFC, there was an 8 m long PNE tube with an inner diameter of 10.8 mm to a gas distribution block made of aluminium with three outlets (ITV, 124 A24 G1/2"). Each outlet had an L-fitting (FESTO, QSL-G1/2-16 186126) and 1.5 m of the same tubing connected to another gas distribution block with eight outlets with a reduction of the tubing diameter to 2.7 mm (FESTO, FR-8-1/4 2078). To each of these outlets an L-fitting (FESTO, QSL-1/4-4 190662) and a 20 m long [tubing](#) with an inner diameter of 2.7 mm PEN tubing (FESTO, PPEN-4X0,75-BL-500 551444) was attached that released the CH₄. At the end of these tubes, no pressure reduction was added. The total pressure drop of the system was expected to be around 0.4 bar.

The pressure and the temperature recorded with the Keller pressure sensor were logged with 10 Hz ([SI-2](#)). From the MFC, the setpoint (L_n min⁻¹), the flow rate (L_n min⁻¹) and the temperature were logged with 0.1 Hz resolution. The MFC had a maximum flow of 160 L_n min⁻¹ and was calibrated for CH₄ at 15 °C. During IC2, the setpoint was varied between 50 and 160 L_n min⁻¹, whereas the flow was kept constant at 140 L_n min⁻¹ during the MC ([SI-2](#)). 140 L_n min⁻¹ correspond to 6.02 kg CH₄ h⁻¹ which represents an emission rate of about 360 dairy cows. ~~Under Swiss regulations, the space in the barn would be insufficient for 360 dairy cows, but~~ This emission rate was chosen to achieve sufficient concentration enhancement at the concentration measurement locations and thus an adequate signal to noise ratio. ~~Under Swiss regulations, the space in the barn would be insufficient for 360 dairy cows.~~ The cumulative flow through the MFC whilst the gas bundle was connected, was within 1% of the CH₄ volume inside the gas bundle.

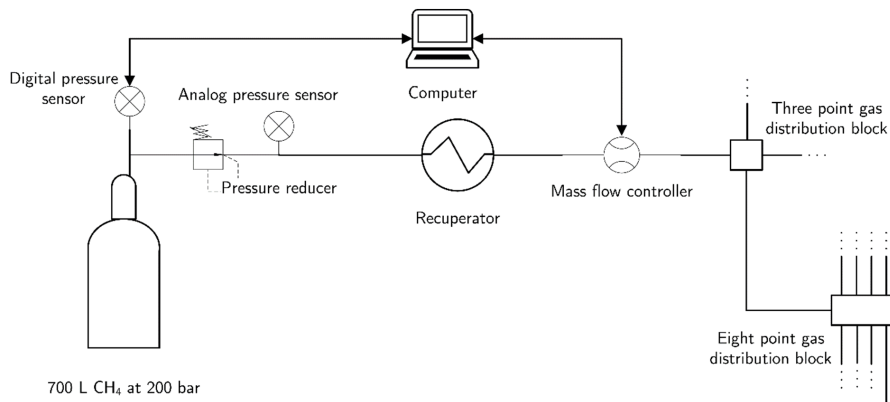


Fig. 2. Schematic of the CH₄ source for the artificial release experiment.

110 The gas bundle and the MFC were placed outside the barn on the north side. The release points inside the barn were at 1.5 m above ground. The 24 release points were equally distributed in the southern half of the barn.

In the beginning of the daytime release in the MC, a short circuit caused a shutdown of the power generator for about 30 min. On 20 March 2021 around 01:00 UTC+1 (nighttime release), the computer was needed to check data from an UA and thus, the CH₄ release was stopped for a few minutes.

115 2.3 Methane concentration measurements

The CH₄ concentrations were measured with five GasFinder3-OP (Boreal Laser Inc., Edmonton, Canada) open-path tunable diode laser absorption spectrometers (hereafter denoted as OP). Twelve-corner cubes mirrors were used as retroreflectors. Data with an insufficient light intensity were removed. Device specific relationships determined by factory calibration were applied to the measured concentration using local air temperature and air pressure measured by a weather station (Lufft WS700-UMB Smart Weather Sensor, G. Lufft Mess- und Regeltechnik GmbH Fellbach, Germany) placed about 100 m southwest from the barn (Fig. 3). The measured CH₄ concentrations (0.3 – 1 Hz resolution) were averaged to 10 min periods and periods with a data coverage lower than 75% (7.5 min) were removed. The concentrations between the five OP were inter-calibrated with data from the parallel measurements in IC1 and IC2 and corrected for slope and offset using linear regression. Afterwards, an additional offset correction was applied based on periods during the MC when no CH₄ was released. The precision for the employed OP was determined from the parallel measurements according to Häni et al. (2021: SI-3).

- Formatted: Subscript
- Formatted: Not Highlight
- Formatted: Not Highlight
- Formatted: , Highlight

Formatted: Font: 6 pt

2.4 Turbulence measurements and data filtering

Four 3D ultrasonic anemometers (UA, Gill Windmaster, Gill Instrument Ltd., Lymington, UK) were used to determine turbulence parameters. A two-axis coordinate rotation was applied ~~for to~~ the wind vector rotation. ~~From the~~The 10 Hz data, ~~were averaged to~~ 10 min periods ~~were built~~.

130 As the ~~dispersion model of the IDMbLS model~~ uses Monin-Obukhov similarity theory (MOST)-scaling, the UA data required compatibility with ~~Monin-Obukhov similarity theory~~ MOST-assumptions and consequently a screening of data with the goal to exclude situations that substantially deviated from ~~these assumptions~~ MOST-conditions. The goal of this screening or quality filtering was to retain as much data as possible without introducing too many erroneous results. Quality filters were applied for the wind direction and the friction velocity u_* . Data with $u_* \leq 0.15 \text{ m s}^{-1}$ were excluded (Flesch et al., 2005b) ~~(Flesch et al., 2005b)~~. ~~The wind direction intervals are given in SI-4~~. No ~~other~~ ~~additional~~ quality filters were applied.

2.5 Experimental setup

For all measurements, the five OP (sensor modules and retroreflectors) were placed 1.60 m above ground level with a path length of 110 m. In IC1, the OP were placed about 100 m southwest of the barn. During the MC, four OP were placed southwest ~~of the barn~~ and one northeast of the barn (Fig. 3) ~~Fig. 3~~. ~~The distance between the barn and the middle of the OP paths on the southwest side were 50 m, 100 m, 150 m, and 200 m. Since the tree located 20 m southwest of the barn was the highest obstacle in the experiment, the locations of the instruments (OP and UA) are indicated as relative distance to the tree (multiple of the tree height $h=15 \text{ m}$) resulting in fetches of 2.0h, 5.3h, 8.6h and 12h. The absolute distance and the corresponding distance as a multiple of the barn height—denoted here as fetch and given in parentheses—between the barn and the middle of the OP path on the southwest side were 50 m (7.1), 100 m (14.3), 150 m (21.4) and 200 m (28.6). Three UA were placed downwind in the middle of the OP paths and one upwind of the barn. The distance between the upwind UA (UA-UW) placed in the northeast of the barn and the trees on the dam in direction of 52° (mean wind direction during release) was 370 m which corresponded to a distance of $>12h$ considering the trees on the dam as dominant height. The measuring heights of all UA was at 2.16 m above ground level. For IC2, all five OP were placed next to each other about 50 m southwest of the barn and one UA was placed 55 m southwest from the barn at 2 m above ground level (Fig. S1, supporting information SI-5).~~

150

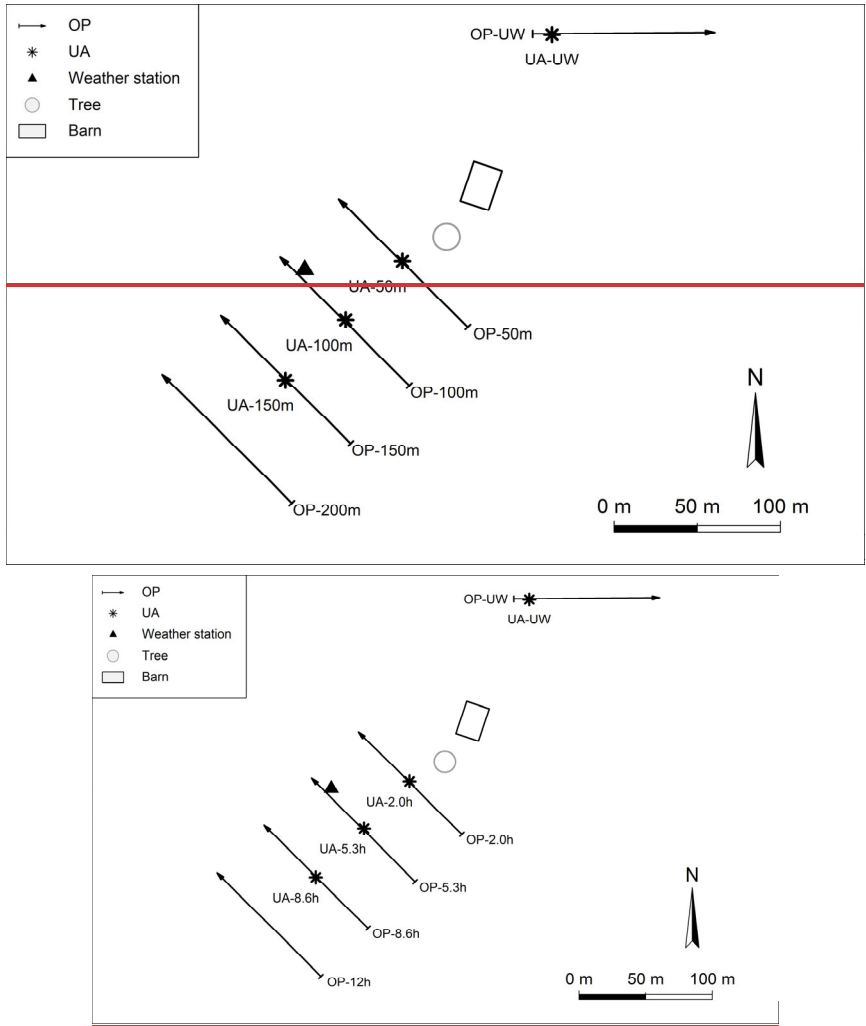


Fig. 3. Schematic overview of the measurement setup during the measurement campaign. OP = open-path device, UA = 3D ultrasonic anemometer, UW = upwind. The numbers behind the OP and UA represent the meters downwind of the barn. The distances as a multiple of the barn height (fetch) are 7.1 for 50 m, 14.3 for 100 m, 21.4 for 150 m and 28.6 for 200 m fetch.

Formatted: Font: 6 pt

155 **2.6 Inverse dispersion method**

~~A backward Lagrangian stochastic (bLS) model was used as atmospheric dispersion model (Flesch et al., 1995; Flesch et al., 2004) was used. The IDM is a micrometeorological approach to measure emissions from a spatially confined source. It uses an atmospheric dispersion model~~ to establish the relationship between the emission of the source and the concentration measured downwind of the source under investigation. This concentration-emission relationship is quantified by the dispersion factor D ($s\ m^{-1}$) which depends on the geometrical configuration of source and concentration sensor as well as on the turbulence and the wind field. To separate the contribution of the source from the incoming (background) concentration at the downwind measurement location, the concentration upwind of the source is ~~equally~~ also measured. With the area A (m^2) of the source, the emission of the source Q ($kg\ s^{-1}$), can be calculated (Eq. 1):

$$Q = \frac{C_{DW} - C_{UW}}{D} \cdot A \quad (\text{Eq. 1})$$

165 where C_{UW} and C_{DW} are the upwind (background) and downwind concentration ($kg\ m^{-3}$).

~~A backward Lagrangian stochastic (bLS) model was used as atmospheric dispersion model (Flesch et al., 1995; Flesch et al., 2004).~~ The bLS model by ~~{Flesch, 2004 #255@@author-year}~~ Flesch et al. (2004) ~~Flesch et al. (1995)~~ uses Monin-Obukhov similarity theory MOST formulas to specify turbulence statistics in the inertial sublayer of the atmosphere, that are derived from the friction velocity, the Obukhov length and the roughness length measured by the UA. Monin-Obukhov similarity theory MOST needs stationarity and homogeneity regarding the turbulence conditions, therefore, the measurement site should be horizontal homogeneous and flat over a large area. Additionally, the bLS model assumes a homogeneous diffusive ground source. A building or a structure violates these conditions and thus based on experimental field trials, it is recommended, that the distance between the source and the downwind measurement locations should be not less than ~~10-ten~~ times the source height so that the turbulence fulfils the assumptions of homogeneity and stationarity (Gao et al., 2010; Harper et al., 2011).

175 The OP in the bLS model were approximated by a series of point sensors with a 1-m spacing along the path length. For each of these point sensors and each emission interval, one million backward trajectories were used to calculate the value of D . The simulations were run in R Statistical Software (v3.6.6: R Core Team 2019) using the package bLSmodelR (Häni et al., 2018), available at <https://github.com/ChHaeni/bLSmodelR>. The following quantities were used as input parameters for the bLS model: the coordinates of the source (barn area), the coordinates of the OP inclusive height above ground, the friction velocity, the Monin-Obukhov length, the roughness height, the wind direction, the standard deviation of the wind direction, the displacement height, the standard deviation of the u , v and w wind divided by friction velocity and the height of the UA above ground.

3 Results

185 A general overview of the weather conditions during the measurement campaign is given in Fig. 4. Due to a change in wind direction, the CH_4 release was stopped for several hours until the conditions were suitable again. During the first part of

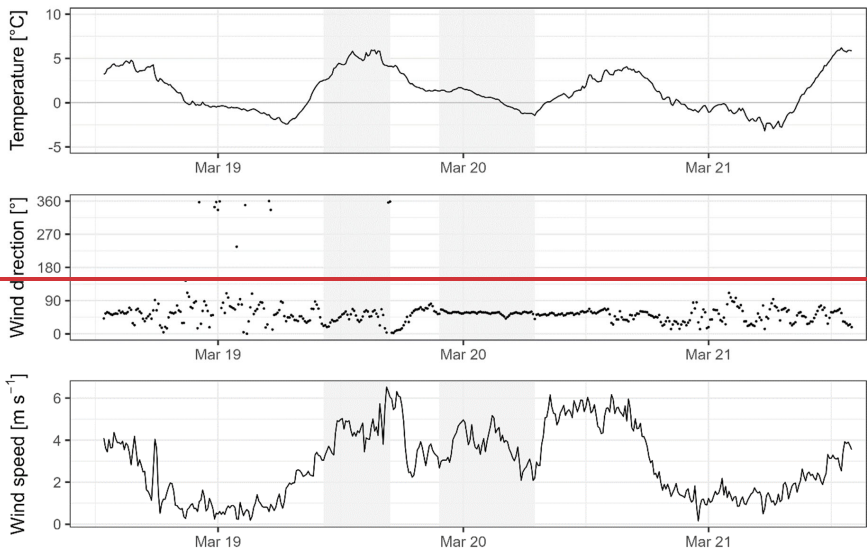
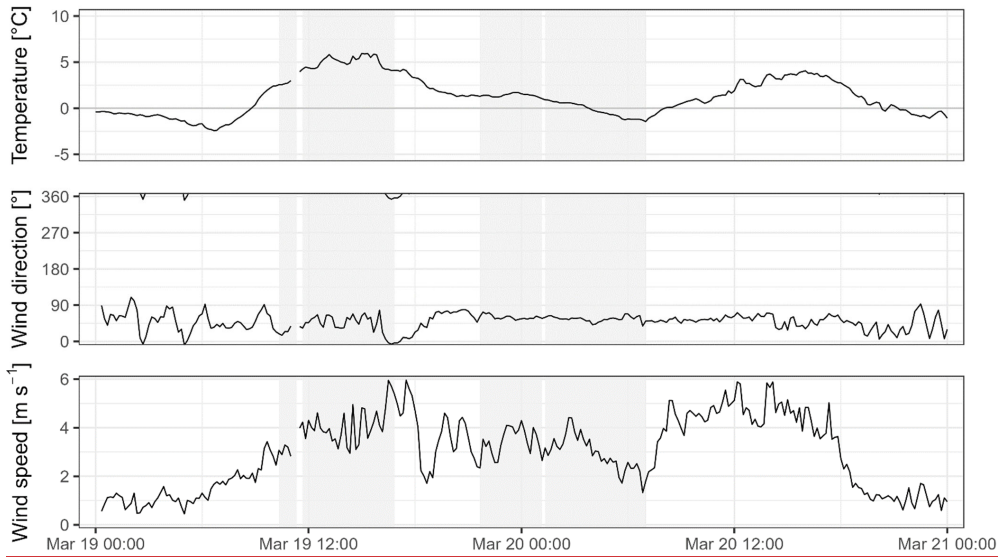
Field Code Changed

Field Code Changed

Formatted: Subscript

Formatted: Font: 6 pt

190 ~~the daytime~~ release the inverse ~~of the~~ Monin-Obukhov length ($1/L$) recorded by UA-UW was between 0 and -0.1 m^{-1} , thus the atmospheric conditions were moderately unstable. ~~In~~ ~~During~~ the ~~second part of the nighttime~~ release, ~~which was mainly during the night,~~ the atmospheric conditions were moderately stable with $1/L$ between 0 and $+0.1 \text{ m}^{-1}$ (~~Fig. S2, supporting information~~ Fig. 5, Table 3). ~~The mean wind direction, the mean wind speed, and the mean friction velocity recorded by UA-UW in the MC during the CH₄ release phases were 51.7°, 3.5 m s⁻¹ and 0.28 m s⁻¹, respectively (Table 3).~~



195

Fig. 4. Weather conditions as 10 min averages measured with the onsite weather station (temperature) and UA-UW (wind direction and wind speed) during the measurement campaign. The grey shaded areas indicate the times during which CH₄ was released.

Formatted: Normal

3.1 Concentration measurements

200

The precision of OP concentration measurements determined during IC1, MC and IC2 ranged between 3.3 and 8.5 ppm-m (Table 1). During the MC, only periods 10 min before and 60 min after a CH₄ release were used to determine the precision. The precision of the OP was lowest during the MC. The median concentration enhancement ($\Delta C = C_{DW} - C_{UW}$) for the daytime and nighttime release are given in Table 2. For these ΔC values, only periods were used, for which also recovery rates were determined. The concentration enhancements were higher during the nighttime release where the atmospheric conditions were stable, than during the daytime release with unstable conditions.

Formatted: Font: 6 pt

205 Table 1. Precision of the OP determined according to Häni et al. (2021). N= number of intervals used to determine precision.

		<u>IC1</u>	<u>MC</u>	<u>IC2</u>	<u>All data</u>
<u>OP-2.0h</u>	<u>Precision [ppm-m]</u>	<u>4.3</u>	<u>5.8</u>	<u>5.9</u>	<u>5.3</u>
	<u>N</u>	<u>695</u>	<u>232</u>	<u>504</u>	<u>1431</u>
<u>OP-5.3h</u>	<u>Precision [ppm-m]</u>	<u>3.3</u>	<u>8.5</u>	<u>4.4</u>	<u>4.4</u>
	<u>N</u>	<u>638</u>	<u>226</u>	<u>505</u>	<u>1369</u>
<u>OP-8.6h</u>	<u>Precision [ppm-m]</u>	<u>5.1</u>	<u>7.1</u>	<u>5.2</u>	<u>5.7</u>
	<u>N</u>	<u>685</u>	<u>228</u>	<u>512</u>	<u>1425</u>
<u>OP-12h</u>	<u>Precision [ppm-m]</u>	<u>4.3</u>	<u>6.3</u>	<u>4.3</u>	<u>4.8</u>
	<u>N</u>	<u>679</u>	<u>226</u>	<u>286</u>	<u>1191</u>

Formatted: Caption_table

Formatted: Centered

Formatted Table

Formatted: Normal

3.2 Recovery rates

210 IDM emissions (Eq. 1) and corresponding recovery rates (IDM emission divided by actual emission according to gas release)
were determined with the different downwind OP instruments using turbulent parameters determined with the UA-UW. During
the CH₄ release, the data loss due to quality filtering was 8%, 11%, 29%, and 36% for OP-2.0h, OP-5.3h, OP-8.6h and OP-
12h, respectively. The resulting recovery rates were always below 1 (Fig. 5). The median recovery rates for the daytime release
during unstable atmospheric condition ranged between 0.57 and 0.61. For the nighttime release during stable atmospheric
conditions, the range was 0.55 – 0.75 (Table 2). The recovery rates for the nighttime release slightly increased with the distance
215 from the OP to the barn/tree, whereas for the daytime release no clear pattern is visible. The highest recovery rates were
achieved under stable atmospheric conditions with the OP furthest away from the source.

Formatted: Font: 6 pt

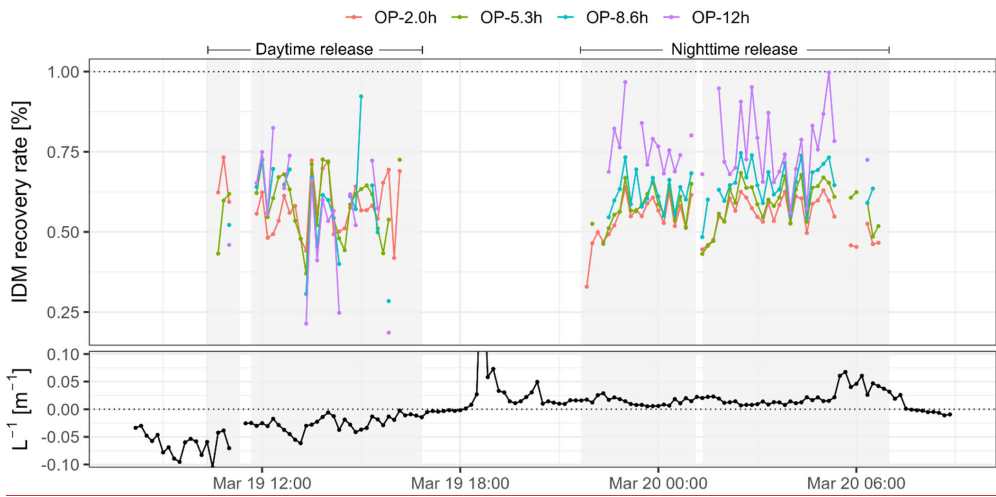


Fig. 5. Top panel: Recovery rate for the measurement campaign. The colours indicate the OP used to calculate the recovery rate. Bottom panel: Atmospheric stability recorded with UA-UW. Grey shaded area are the times as CH₄ was released. The time series is in UTC+1.

220

Formatted: Keep with next

Formatted: Caption

Formatted: Subscript

Formatted: Font: 6 pt

Table 2. Median recovery rates with standard deviation, median concentration enhancements (ΔC) with standard deviation, and number of 10 min intervals (N) for all OP using the data from UA-UW for the two releases in the MC. Daytime release (unstable atmospheric conditions), nighttime release (stable atmospheric conditions).

OP		Daytime release ($L < 0$)	Nighttime release ($L > 0$)	Entire MC
	Recovery rate	0.57±0.09	0.55±0.06	0.56±0.07
OP-2.0h	ΔC [ppm-m]	58.4±12.9	78.3±16.9	70.7±17.8
	N	30	50	80
	Recovery rate	0.61±0.10	0.59±0.06	0.59±0.08
OP-5.3h	ΔC [ppm-m]	33.2±8.4	49.8±12.3	43.5±14.9
	N	29	48	77
	Recovery rate	0.61±0.15	0.64±0.06	0.63±0.10
OP-8.6h	ΔC [ppm-m]	21.2±4.8	36.1±10	30.4±11.7
	N	20	42	62
	Recovery rate	0.57±0.18	0.75±0.10	0.71±0.17
OP-12h	ΔC [ppm-m]	12.9±4.4	27.6±8.6	22.1±10.9
	N	19	37	56

3.4.3 Influence of the barn and the tree on the wind field on the wind field

The wind directions of the downwind UA instruments showed systematic deviations from the UA-UW for the wind sector deviated between 40° and 65° from the UA-UW with a maximum deviation at around 55° (Fig. 6Fig-5). The barn was located at 45° of the downwind UA locations and 225° of the UA-UW, respectively (Fig. 3). The closer the downwind UA was placed to the barn, the further the local wind direction deviated towards north from the upwind wind direction measured by UA-UW (Table 3Table-4). A similar pattern can be seen was found for the u_x values. For the standard deviation of the v wind divided by friction velocity, the deviations between the UA-UW and the downwind UA are strongest for the 50 m location. For UA-100m and UA-150m there is a constant offset of 0.49 (Fig. S4, supporting informationSI-6). The observed atmospheric stability was very similar for all UA (Table 3). Emission recovery rates determined with the UA placed downwind of the barn, can be found in the supporting information (SI-7).

Formatted: Caption_table

Formatted

Formatted: Centered

Formatted: Font: (Default) CMU Serif, 8 pt, Font color: Black, German (Switzerland)

Formatted: Centered

Formatted Table

Formatted: Normal

Formatted: Heading 3

Formatted: Font: 6 pt

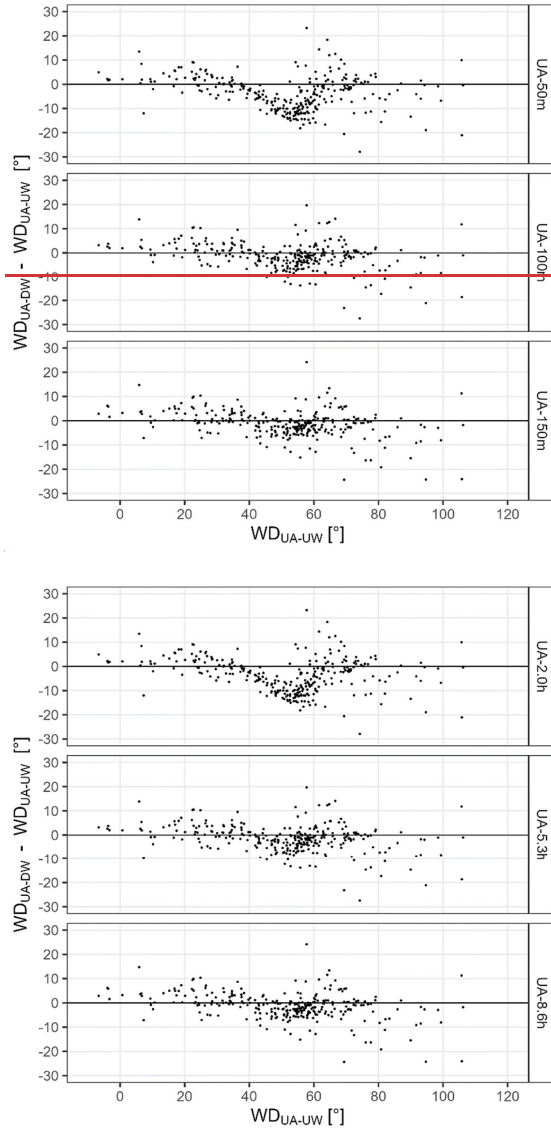


Fig. 65. Absolute difference in the wind direction between the three downwind UA (UA-DW) and the upwind UA (UA-UW) recorded during the entire measurement campaign given as 10-min data. The exact locations of the UA are given in Fig. 3.

The wind speed of the UA closest to the barn was, depending on the wind direction, either higher or lower than the wind speed measured with the UA-UW (Fig. S3, supporting information). At 150 m from the barn, the wind speed was on average 7% higher than at the upwind location. A similar pattern can be seen for the u_z values. For the standard deviation of the v wind divided by friction velocity, the deviations between the UA-UW and the downwind UA are strongest for the 50 m location. For UA-100m and UA-150m there is a constant offset of 0.49 (Fig. S4, supporting information).

Table 3. Mean wind direction (WD), mean wind speed (WS), mean friction velocity (u_z) and the mean of the inverse of the Obukhov length (L^{-1}) recorded of the four by the UA during the two release phases in the MC measurement campaign and while CH₄ was released in the measurement campaign.

	During measurement campaign Daytime release				During CH ₄ release Nighttime release			
	Mean-WD [°]	Mean-WS [m s ⁻¹]	Mean- u_z [m s ⁻¹]	L^{-1} [m ⁻¹]	Mean-WD [°]	Mean-WS [m s ⁻¹]	Mean- u_z [m s ⁻¹]	L^{-1} [m ⁻¹]
UA-UW	43.05±1.6	4.02±.6	0.320±19	-0.03	58.15±1.6	3.23±.5	0.250±.28	0.02
UA-50m 2.0h	41.146±.7	3.93±.9	0.310±.23	-0.03	50.445±.8	2.73±.2	0.220±.25	0.05
UA-100m 5.3h	43.95±0.4	4.22±.7	0.360±.22	-0.02	55.950±.7	3.23±.6	0.300±.32	0.02
UA-150m 8.6h	44.55±0.8	4.32±.9	0.370±.23	-0.02	55.450±.7	3.53±.8	0.290±.32	0.02

3.2 Recovery rates

During the MC whilst CH₄ was being released, the data loss due to quality filtering was highest with the combination UA-50m and OP-200m (40%) and lowest with UA-100m and OP-50m (5%). On average, UA-100m, UA-150m and UA-UW showed similar data loss, whereas the data loss for UA-50m was a bit higher (Table 2). The recovery rates (determined emission divided by actual emission) determined from the different UA and OP combinations were on average always below 1 and did not substantially differ during the MC (Table 3, Fig. 6). The median recovery rates ranged between 0.56–0.71. The median recovery rate slightly increases with the distance from the OP to the barn for all UA, except for UA-50m.

Table 2 Percentage of data loss of the different UA and OP combinations after quality filtering during the MC whilst being gas was released.

	UA-UW	UA-50m	UA-100m	UA-150m
OP-50m	8%	16%	5%	6%
OP-100m	11%	21%	9%	11%
OP-150m	29%	32%	24%	22%

Formatted: Line spacing: 1.5 lines

Formatted Table

Formatted: Line spacing: 1.5 lines

Formatted: Right, Line spacing: 1.5 lines

Formatted: Line spacing: 1.5 lines

Formatted: Line spacing: 1.5 lines

Formatted: Line spacing: 1.5 lines

Formatted: Line spacing: 1.5 lines

Formatted: Heading 3

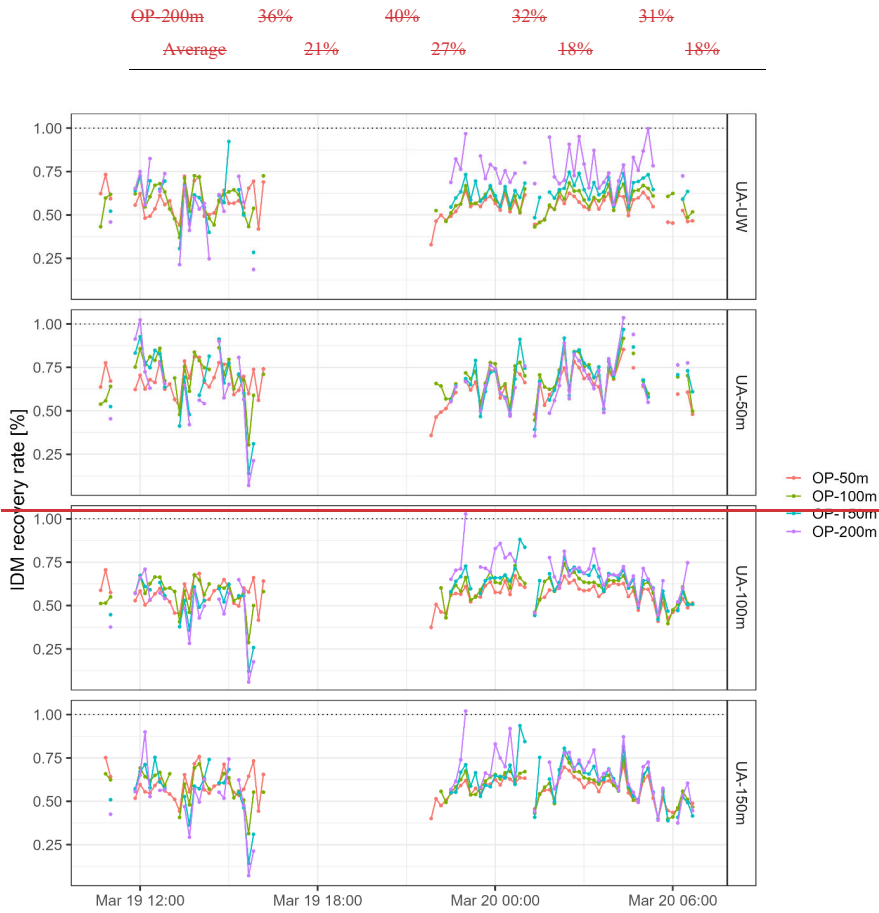
Formatted: Normal

Formatted: Normal

Formatted: Normal

Formatted: Normal

Formatted: Font: 6 pt



- Formatted: Normal
- Formatted: Normal, Centered
- Formatted Table
- Formatted: Normal, Centered

Fig. 6 Recovery rate for the measurement campaign with all possible UA and OP combinations. Each panel represents an UA and the colours indicates the OP used to calculate the recovery rate. The time series is in UTC+1.

Formatted: Centered

265

Table 3: Median recovery rates for all possible OP-UA combinations for the MC whilst being CH released.

	UA-50m	UA-100m	UA-150m
--	--------	---------	---------

Formatted: Font: 6 pt

OP-50m	0.65	0.58	0.58
OP-100m	0.70	0.60	0.60
OP-150m	0.69	0.62	0.61
OP-200m	0.65	0.66	0.62
All OP	0.67	0.60	0.60

Formatted: Centered

Formatted: Centered

Formatted: Centered

Formatted: Centered

Formatted: Centered

Formatted: Heading 1

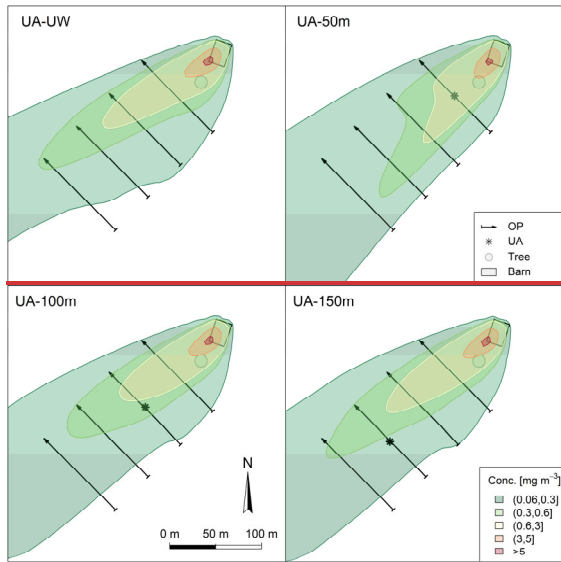
3.3 Plume modelling and wind field rotation

With the bLS model it is also possible to model an emission plume by calculating the dispersion factor D for every point of a grid laid over the experimental site. For each of the grid points, the expected concentration with the given emission of 6.02 kg CH₄ h⁻¹, is calculated which allows to establish a contour plot (Fig. 7). For all UA most of the modelled

270

Formatted: Font: 6 pt

emission plume is within the measurement path of the OP. For UA-UW, UA-100m and UA-150m, the average plume is slightly shifted towards the northwest end of the OP path.



275 **Fig. 7** Contours of the averages overall modelled emission plumes given as concentration enhancements for the xy-plane at a height of 1.60 m above ground for the bLS runs based on the four UA. The name of the OP and the position of the UA-UW are given in Fig. 3.

280 Next to that visualisation, also implications on the recovery rates by rotating the wind field by 10° clock and anticlockwise in 1° steps were tested (Fig. 8). The emissions of the OP closest to the barn was almost unaffected by any change in wind direction. The more the OP was placed away from the barn, the larger were the changes in emissions

Formatted: Font: 6 pt

due to the wind field rotation. Generally, a clockwise shift of the wind field led to higher emissions and an anticlockwise shift led unchanged or lower emission estimates, whereas the changes were more pronounced with a clockwise rotation.

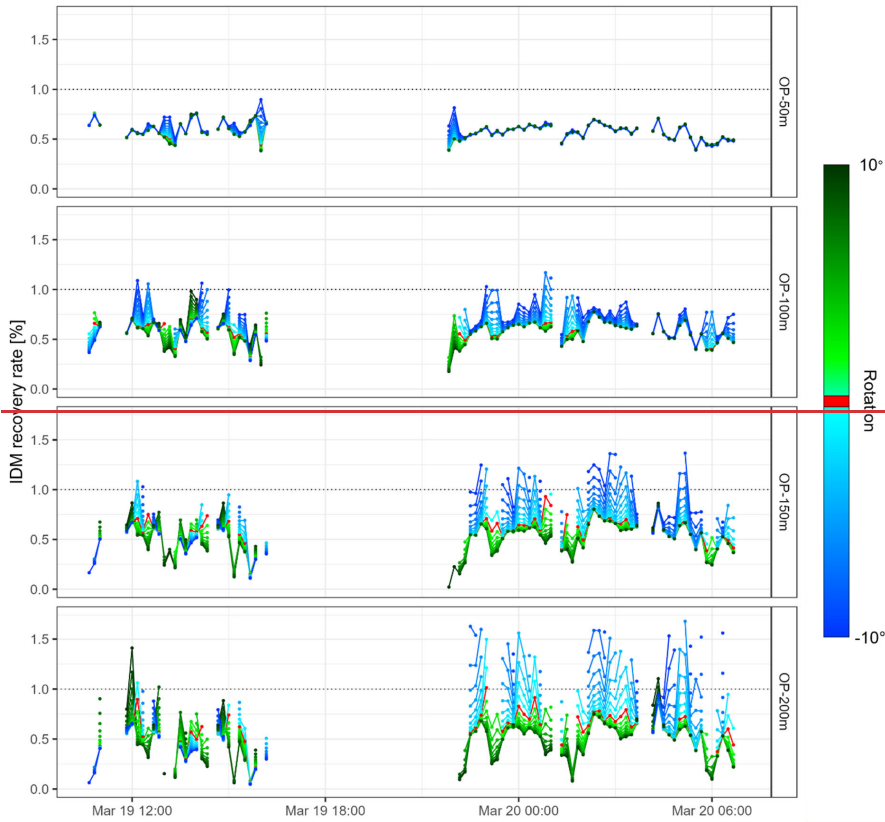


Fig. 8 Effects of the wind field rotation on the IDM recovery rate calculated with UA-150m and the four downwind OP. Each colour represents a rotation by 1°. Green: anticlockwise rotation of the wind field. Blue: clockwise rotation of the

285

Formatted: Font: 6 pt

~~wind field. Red: original line. The time series is in UTC+1. Note that due to wind direction filtering (for every run the same) not every run has the same number of data points.~~

4 Discussion

4.1 Influence of the barn on the wind field

290 The influence of the barn and the tree ~~on the measured on-the~~ downwind turbulence ~~measurements~~ is clearly visible (Fig. 6, Table Table 2Table 3). The closer the UA was placed to the ~~tree and the~~ barn, the larger was the influence. The wind must flow around the barn ~~and the tree~~ and thus the largest deviation in the wind direction was measured at around 55°, which corresponds to the southwest-northeast diagonal of the barn. The wind field deviation is also visible in all other turbulence parameters (Fig. S4, supporting informationSI-6). ~~The wind speed of the downwind UA closest to the barn was, depending~~
295 ~~on the wind direction, either higher or lower than the wind speed measured by the UA-UW (SI-8). At UA-5.3h and UA-8.6h,~~ the wind speed and friction velocity were on average slightly higher than at the upwind location, independent of the atmospheric stability. Even though some of the devices were placed at a downwind distance of more than the recommended 10 times the barn height away (Harper et al., 2011, Gao et al., 2010), a deviation of the wind direction of the downwind UA compared to the UA-UW due to the barn was still visible at 100 m (fetch = 14.3 times barn height) and 150 m (fetch = 21.4).
300 However, if the 15 m high tree is considered as relevant flow disturbance, the fetch values become considerable smaller, namely 2.0, 5.3, 8.6 and 12.0 for the instrument locations at 50 m, 100 m, 150 m and 200 m, respectively (see Fig. 3).
The difference in the turbulence parameters indicate that ~~all the downwind the~~ UA (fetch between 2.0h - 8.6h) were still in the wake of the barn and the tree. This wind field deviation ~~will~~ most likely ~~led to a deviateion of the actual emission plume dispersion~~ from the ~~dispersion calculated from simulations by~~ the bLS model, but unfortunately, ~~the resulting deviation in the~~ calculated IDM emission cannot be quantified and corrected ~~for we cannot model that. Consequently, the calculated recovery rates will have a deviation from the expected values.~~

4.2 Quality filtering and data loss

In this ~~measurement campaignstudy~~, a minimum of quality filters was applied. Compared to other measurement campaigns conducted in Switzerland (Bühler et al., 2022; Bühler et al., 2021), this ~~measurement~~ campaign was of shorter duration and
310 the atmospheric conditions ~~were varied lessmore favourable for emission quantification~~. Additional filters, other than ~~filtering for u_x~~ , and the wind direction, were tested but not applied in the final analysis, since they excluded more data but did not alter the findings and the mean and median recovery rates.

4.3 Recovery rates

The recovery ~~rates of the IDM emission resultsrates for the UA, except UA-50m,~~ slightly increased with the distances of the
315 ~~downwind~~ OP to the barn ~~for the nighttime release. For both release phases and for all fetches (2.0h – 12h), the median recovery~~

rate did not exceed 0.75. On the other hand, there is no pattern in the recovery rate in terms of increasing distance of the UA from the barn (Fig. S5, supporting information). The recovery rates of the OP closest to the barn are consistent with the findings of Gao et al. (2010), who conducted a similar experiment released CH₄ via side vents at a barn, and achieved a recovery rate of 0.66 for a fetch similar to that of 5h. However, for a fetch of 10h to 25h times the building height, Gao et al. (2010) measured recovery rates between 0.93 and 1.03 while in the present study the median recovery rate for similar fetches (considering the barn as highest point) remained between 0.59 and 0.71. McGinn et al. (2006) determined recovery rates between 0.59 and 1.05 with an average of 0.86 for a fetch of 9h and larger. For a fetch of 10h at a biogas plant, Hrad et al. (2021) measured a recovery rate of 1.19 (variant 1, USA A). Baldé et al. (2016) released CH₄ on the slurry surface of two storage tanks and got recovery rates ranging from 0.91 to 1.20 with an average of 1.05. But unfortunately, it was not possible to determine a fetch from the given data. Among the above-mentioned studies, the one by Gao et al. (2010) is the most comparable to our study.

The often proposed and used minimum fetch of 10h for the positioning of downwind concentration measurements might not always be sufficient. In our study, at a fetch of 12h, the observed recovery rates showed a median of 0.57 and 0.75 and were never above 1. This suggests that the fetch of 12h from the flow disturbing obstacle was not enough in this case. However, from the available data in our study, it is not possible to state that longer fetches would considerably improve the recovery rate. This is in line with the statement of Flesch et al. (2005a) that the determination of an universal distance for a fetch that reliably avoids wind disturbances is unlikely.

Nevertheless, we tried to rule out or explain possible mechanism for the low recovery rates. A bias in the release rate that could explain them is unlikely, as the

he cumulative flow through the MFC was within 1% of the CH₄ volume inside the gas bundle. The precision of the OP were comparable to the values presented by Häni et al. (2021) for intercomparisons with similar path lengths. Based on Häni et al. (2021), the high CH₄ release rate of 140 L_a min⁻¹ was chosen in the present study to achieve a suitable signal to noise ratio. This was generally accomplished, as for the OP-12h, the precision was 26% of the median concentration enhancement. In the nighttime release, where the highest recovery rates were determined, the concentration enhancement for OP-12h was even larger and the precision generally below 23%. Thus, to the best of our knowledge, biases in the intercalibration of the OP instruments or in the amount of released gas cannot explain the low IDM recovery rates. A bias in the results due to biases in the intercalibration of the OP or in the amount of released gas could be excluded. Therefore, it is likely that the deviations of the modelled dispersion by the applied bLS model from real conditions are mainly responsible for the lower IDM recovery rates.

When the barn was excessively vented after the CH₄ release, no increase in the downwind CH₄ concentration could be observed, indicating that no CH₄ was kept back inside the barn. On the other hand, there is no pattern in the recovery rate in terms of increasing distance of the UA from the barn (Fig. S5, supporting information).

Even though the wind direction deviated by 7° from the expected wind direction, most of the averaged modelled emission plume was still within the open path measurements (Fig. 7). However, the results from the wind field rotation indicate that the

Formatted: Subscript

Formatted: Subscript

Formatted: Not Highlight

Formatted: Not Highlight

Formatted: Not Highlight

Formatted: Subscript

Formatted: Not Highlight

Formatted: Not Highlight

Formatted: Font: 6 pt

350 modelled emission plume was rather on the edge of the OP measurement paths. Nevertheless, those modulations cannot explain the low recovery rate. There are multiple time intervals where the rotation of the wind field had no effect on the recovery rate and that recovery rate remained distinctly below 1, indicating that an offset in the model wind direction cannot be the sole reason.

355 Despite promising experimental conditions and having the experiment carefully executed, the experiment such as long measurement paths - the use of path integrated concentration measurements is much less sensitive to biases in the wind direction than point measurements (Häni et al., submitted) -, relatively long fetches, high release rates were used, and the terrain was being relatively approximately horizontal, homogeneous and flat, the recovery rates were lower than expected. The low recovery rates indicate that the mixing of the released CH₄ into the atmosphere was larger than in the bLS model world. This larger mixing could have been in any of the three dimensions. As lateral and vertical mixing are coupled and any changes in one direction has consequences in the two others, disentangling is difficult.

360 Nevertheless, a possible explanation for the lower recovery rates is that the initial vertical mixing of the CH₄ was larger than in the bLS model. Such a larger mixing can occur, because the bLS model assumes a diffusive ground source which releases gas into an ideal flow field. In our case, the gas CH₄ was actively released inside the barn about 1.5 m above ground and might have left the barn at an even higher height above ground and thus, the initial vertical displacement of the CH₄ could have led to lower emission estimates since the bLS model assumes a diffusive ground source. More importantly, also, the flow distortion wake caused by the barn and its interaction with the nearby tree could have led to an strong updraft resulting in and consequently increased vertical mixing of the plume.

370 To verify this hypothesis, a vertical profile of the CH₄ concentrations inside the plume at the same OP locations would provide insight on changes in the have been necessary recovery rates with height. Expected are increasing recovery rates with increasing height. Additionally, an analysis of the plume shape via a drone or a mobile high resolution measurement device could give qualitative information on concentration profile at the release from the building and would add to a better interpretation of the IDM emission data.

375 Thus, with using the bLS model and the IDM, it is more likely to underestimate emissions than overestimating them. However, it is not possible to conclude from the present study how many times underestimation of housing emissions determined with a bLS model occur, as there were studies showing good results with the bLS model in comparable situations (Bühler et al., 2021; Gao et al., 2010).

5 Conclusions

380 The median IDM recovery rates of the release experiment were 0.565 - 0.745 and thus, smaller than 1, which cannot be conclusively explained conclusively. We hypothesise that the barn and the tree in the main wind axis have led to the systematic underestimation of the IDM-derived emission rates due to the deviations of the wind field and turbulent dispersion from the ideal assumptions in the bLS model. However, information regarding the shape of the plume was not available. It is important

Formatted: Subscript

Formatted: Subscript

Formatted: Font: 6 pt

to note that the present study does not provide conclusive evidence that the IDM with the used IDM-bLS model generally underestimates barn emissions. In our study at a fetch of 12h, we were still in the disturbed zone from the barn and the tree. Other IDM studies using the applied bLS model have shown near 100% recovery with comparable fetches for similar release experiments or good agreement with with an independent reference method. Thus, there is no universally valid minimum distance, at which one must place the concentration measurements downwind of a source to obtain accurate results. However, mMore experiments with controlled gas releases (including the tracer ratio method) inside, where the target gas is released inside a barn would be desirable for validation, or a tracer ratio method is used as validation, might be needed to better understand the limitations of the IDM. Additional downwind Our recommendations for barn measurements with IDM are that despite following all recommendations, there is no 100% guarantee that the IDM will provide accurate emission results. Therefore, we recommend that experiments be carried out carefully and one should be aware that deviations might occur. Downwindvertical profile measurements of the concentration or a qualitative plume mapping with a drone or a mobile high resolution measurement device might help to detect deviations in shape of the dispersion plumessee if such deviations occur.

Formatted: Not Highlight

Formatted: Not Highlight

Formatted: Not Highlight

Author contributions

TK was responsible for funding acquisition; MB, CH and TK were for responsible for conceptualisation; MB and PB were responsible for conducting the CH₄ release; MB and CH were responsible for data evaluation; MB was responsible for the visualisation; MB was responsible for writing the original draft with essential inputs from CH, AN, CA and TK.

Competing interests

At least one of the co-authors is a member of the editorial board of Atmospheric Measurement Techniques.

Data

The treated data of the MC and IC2 can be found in the supporting information. More information on data availability is provided in SI-9.

Acknowledgements

Funding from the Swiss Federal Office for the Environment (Contract number: 00.5082.PZ/BECDD68E6) is gratefully acknowledged. We thank the owner of the barn and farmers of the land in the surrounding areas for their collaboration and assistance. We thank Simon Bowald for the planning of the CH₄ source and Simon Bowald and Martin Häberli-Wyss for their support during the measurements (both School of Agricultural, Forest and Food Sciences, Zollikofen).

Formatted: Font: 6 pt

References

- 410 [Arias, P., Bellouin, N., Coppola, E., Jones, R., Krinner, G., Marotzke, J., Naik, V., Palmer, M., Plattner, G.-K., Rogelj, J., Rojas, M., Sillmann, J., Storelvmo, T., Thorne, P., Trewin, B., Rao, K., Adhikary, B., Allan, R., Armour, K., and Zickfeld, K.: IPCC AR6 WGI Technical Summary, in, 33-144, <https://doi.org/10.1017/9781009157896.002>, 2021.](#)
- 415 [Baldé, H., VanderZaag, A. C., Burt, S., Evans, L., Wagner-Riddle, C., Desjardins, R. L., and MacDonald, J. D.: Measured versus modeled methane emissions from separated liquid dairy manure show large model underestimates, *Agriculture, Ecosystems & Environment*, 230, 261-270, <https://doi.org/10.1016/j.agee.2016.06.016>, 2016.](#)
- 420 [Bühler, M., Häni, C., Ammann, C., Brönnimann, S., and Kupper, T.: Using the inverse dispersion method to determine methane emissions from biogas plants and wastewater treatment plants with complex source configurations, *Atmospheric Environment: X*, 13, 100161, <https://doi.org/10.1016/j.aecoa.2022.100161>, 2022.](#)
- 425 [Bühler, M., Häni, C., Ammann, C., Mohn, J., Neftel, A., Schrade, S., Zähler, M., Zeyer, K., Brönnimann, S., and Kupper, T.: Assessment of the inverse dispersion method for the determination of methane emissions from a dairy housing, *Agricultural and Forest Meteorology*, 307, 108501, <https://doi.org/10.1016/j.agrformet.2021.108501>, 2021.](#)
- 430 [Flesch, T. K., Wilson, J. D., and Harper, L. A.: Deducing ground-to-air emissions from observed trace gas concentrations: A field trial with wind disturbance, *Journal of Applied Meteorology*, 44, 475-484, <https://doi.org/10.1175/Jam2214.1.2005a>.](#)
- 435 [Flesch, T. K., Wilson, J. D., and Yee, E.: Backward-Time Lagrangian Stochastic Dispersion Models and Their Application to Estimate Gaseous Emissions, *Journal of Applied Meteorology*, 34, 1320-1332, \[https://doi.org/10.1175/1520-0450\\(1995\\)034<1320:Btldsm>2.0.Co;2\]\(https://doi.org/10.1175/1520-0450\(1995\)034<1320:Btldsm>2.0.Co;2\), 1995.](#)
- 440 [Flesch, T. K., Harper, L. A., Powell, J. A., and Wilson, J. D.: Inverse-Dispersion Calculation of Ammonia Emissions from Wisconsin Dairy Farms, *Transactions of the Asabe*, 52, 253-265, <https://doi.org/10.13031/2013.25946>, 2009.](#)
- 445 [Flesch, T. K., Wilson, J. D., Harper, L. A., and Crenna, B. P.: Estimating gas emissions from a farm with an inverse-dispersion technique, *Atmospheric Environment*, 39, 4863-4874, <https://doi.org/10.1016/j.atmosenv.2005.04.032.2005b>.](#)
- [Flesch, T. K., Wilson, J. D., Harper, L. A., Crenna, B. P., and Sharpe, R. R.: Deducing ground-to-air emissions from observed trace gas concentrations: A field trial, *Journal of Applied Meteorology*, 43, 487-502, \[https://doi.org/10.1175/1520-0450\\(2004\\)043<0487:Dgefot>2.0.Co;2\]\(https://doi.org/10.1175/1520-0450\(2004\)043<0487:Dgefot>2.0.Co;2\), 2004.](#)
- 435 [Gao, Z. L., Desjardins, R. L., and Flesch, T. K.: Assessment of the uncertainty of using an inverse-dispersion technique to measure methane emissions from animals in a barn and in a small pen, *Atmospheric Environment*, 44, 3128-3134, <https://doi.org/10.1016/j.atmosenv.2010.05.032>, 2010.](#)
- 440 [Gerber, P. J., Steinfeld, H., Henderson, B. B., Mottet, A., Opio, C. I., Dijkman, J., Falcucci, A., and Tempio, G.: Tackling climate change through livestock - A global assessment of emissions and mitigation opportunities, *Food and Agricultural Organization of the United Nations \(FAO\)*, Rome, 2013.](#)
- 445 [Häni, C., Bühler, M., Neftel, A., Ammann, C., and Kupper, T.: Performance of open-path GasFinder3 devices for CH4 concentration measurements close to ambient levels, *Atmospheric Measurement Techniques*, 14, 1733-1741, <https://doi.org/10.5194/amt-14-1733-2021>, 2021.](#)
- [Häni, C., Flechard, C., Neftel, A., Sintermann, J., and Kupper, T.: Accounting for Field-Scale Dry Deposition in Backward Lagrangian Stochastic Dispersion Modelling of NH3 Emissions, *Atmosphere*, 9, 146, <https://doi.org/10.3390/atmos9040146>, 2018.](#)
- [Häni, C., Neftel, A., Flechard, C., Amman, C., Valach, A., and Kupper, T.: Validation of a short-range dispersion and deposition model using field-scale ammonia and methane release experiments, *Agricultural and Forest Meteorology*, submitted.](#)

Formatted: German (Switzerland)

Formatted: References

Formatted: Font: 6 pt

- 450 [Harper, L. A., Denmead, O. T., and Flesch, T. K.: Micrometeorological techniques for measurement of enteric greenhouse gas emissions. *Animal Feed Science and Technology*, 166-67, 227-239, <https://doi.org/10.1016/j.anifeedsci.2011.04.013>, 2011.](#)
- [Hrad, M., Vesenmaier, A., Flandorfer, C., Piringner, M., Stenzel, S., and Huber-Humer, M.: Comparison of forward and backward Lagrangian transport modelling to determine methane emissions from anaerobic digestion facilities. *Atmospheric Environment-X*, 12, 100131, <https://doi.org/10.1016/j.aeaoa.2021.100131>, 2021.](#)
- 455 [Laubach, J., Bai, M., Pinares-Patino, C. S., Phillips, F. A., Naylor, T. A., Molano, G., Rocha, E. A. C., and Griffith, D. W. T.: Accuracy of micrometeorological techniques for detecting a change in methane emissions from a herd of cattle. *Agricultural and Forest Meteorology*, 176, 50-63, <https://doi.org/10.1016/j.agrformet.2013.03.006>, 2013.](#)
- 460 [McGinn, S. M., Flesch, T. K., Harper, L. A., and Beauchemin, K. A.: An approach for measuring methane emissions from whole farms. *J Environ Qual*, 35, 14-20, <https://doi.org/10.2134/jeq2005.0250>, 2006.](#)
- [Saunio, M., Stavert, A. R., Poulter, B., Bousquet, P., Canadell, J. G., Jackson, R. B., Raymond, P. A., Dlugokencky, E. J., Houweling, S., Patra, P. K., Chai, S., Arora, V. K., Bastviken, D., Bergamaschi, P., Blake, D. R., Brailsford, G., Bruhwiler, L., Carlson, K. M., Carrol, M., Castaldi, S., Chandra, N., Crevoisier, C., Crill, P. M., Covey, K., Curry, C. L., Etiopie, G., Frankenberg, C., Gedney, N., Hegglin, M. I., Hoglund-Isaksson, L., Hugelius, G., Ishizawa, M., Ito, A., Janssens-Maenhout, G., Jensen, K. M., Joos, F., Kleinen, T., Krummel, P. B., Langenfelds, R. L., Laruelle, G. G., Liu, L. C., Machida, T., Maksyutov, S., McDonald, K. C., McNorton, J., Miller, P. A., Melton, J. R., Morino, I., Muller, J., Murguia-Flores, F., Naik, V., Niwa, Y., Noce, S., Doherty, S. O., Parker, R. J., Peng, C. H., Peng, S. S., Peters, G. P., Prigent, C., Prinn, R., Ramonet, M., Regnier, P., Riley, W. J., Rosentretter, J. A., Segers, A., Simpson, I. J., Shi, H., Smith, S. J., Steele, L. P., Thornton, B. F., Tian, H. Q., Tohjima, Y., Tubiello, F. N., Tsuruta, A., Viovy, N., Voulgarakis, A., Weber, T. S., van Weele, M., van der Werf, G. R., Weiss, R. F., Worthy, D., Wunch, D., Yin, Y., Yoshida, Y., Zhang, W. X., Zhang, Z., Zhao, Y. H., Zheng, B., Zhu, Q., Zhu, Q. A., and Zhuang, Q. L.: The Global Methane Budget 2000-2017. *Earth System Science Data*, 12, 1561-1623, <https://doi.org/10.5194/essd-12-1561-2020>, 2020.](#)
- 470 [Sommer, S. G., Christensen, M. L., Schmidt, T., and Jensen, L. S.: *Animal Manure Recycling*. John Wiley & Sons, Ltd, Chichester, UK, <https://doi.org/10.1002/9781118676677>, 2013.](#)
- [VanderZaag, A. C., Flesch, T. K., Desjardins, R. L., Balde, H., and Wright, T.: Measuring methane emissions from two dairy farms: Seasonal and manure-management effects. *Agricultural and Forest Meteorology*, 194, 259-267, <https://doi.org/10.1016/j.agrformet.2014.02.003>, 2014.](#)
- 480 [Baldé, H., VanderZaag, A. C., Burt, S., Evans, L., Wagner-Riddle, C., Desjardins, R. L., and MacDonald, J. D.: Measured versus modeled methane emissions from separated liquid dairy manure show large model underestimates. *Agriculture, Ecosystems & Environment*, 230, 261-270, \[10.1016/j.agee.2016.06.016\]\(https://doi.org/10.1016/j.agee.2016.06.016\), 2016a.](#)
- [Baldé, H., VanderZaag, A. C., Burt, S. D., Wagner-Riddle, C., Crolla, A., Desjardins, R. L., and MacDonald, D. J.: Methane emissions from digestate at an agricultural biogas plant. *Bioresource Technology*, 216, 914-922, \[10.1016/j.biortech.2016.06.031\]\(https://doi.org/10.1016/j.biortech.2016.06.031\), 2016b.](#)
- 485 [Bühler, M., Häni, C., Ammann, C., Mohn, J., Neftel, A., Schrade, S., Zähler, M., Zeyer, K., Brönnimann, S., and Kupper, T.: Assessment of the inverse dispersion method for the determination of methane emissions from a dairy housing. *Agricultural and Forest Meteorology*, 307, 108501, \[10.1016/j.agrformet.2021.108501\]\(https://doi.org/10.1016/j.agrformet.2021.108501\), 2021.](#)
- [Bühler, M., Häni, C., Ammann, C., Brönnimann, S., and Kupper, T.: Using the inverse dispersion method to determine methane emissions from biogas plants and wastewater treatment plants with complex source configurations. *Atmospheric Environment: X*, 13, 100161, \[10.1016/j.aeaoa.2022.100161\]\(https://doi.org/10.1016/j.aeaoa.2022.100161\), 2022.](#)
- 490 [Flesch, T. K., Wilson, J. D., and Yee, E.: Backward-time Lagrangian stochastic dispersion models and their application to estimate gaseous emissions. *Journal of Applied Meteorology*, 34, 1320-1332, \[Doi 10.1175/1520-0450\\(1995\\)034<1320:Btldsm>2.0.Co;2\]\(https://doi.org/10.1175/1520-0450\(1995\)034<1320:Btldsm>2.0.Co;2\), 1995.](#)
- 495 [Flesch, T. K., Wilson, J. D., Harper, L. A., Crenna, B. P., and Sharpe, R. R.: Deducing ground-to-air emissions from observed trace gas concentrations: A field trial. *Journal of Applied Meteorology*, 43, 487-502, \[Doi 10.1175/1520-0450\\(2004\\)043<0487:Dgefot>2.0.Co;2\]\(https://doi.org/10.1175/1520-0450\(2004\)043<0487:Dgefot>2.0.Co;2\), 2004.](#)

- Flesch, T. K., Wilson, J. D., Harper, L. A., and Crenna, B. P.: Estimating gas emissions from a farm with an inverse dispersion technique, *Atmospheric Environment*, 39, 4863–4874, 10.1016/j.atmosenv.2005.04.032, 2005.
- 500 Flesch, T. K., Harper, L. A., Powell, J. A., and Wilson, J. D.: Inverse dispersion calculation of ammonia emissions from Wisconsin dairy farms, *Transactions of the ASABE*, 52, 253–265, 10.13031/2013.25946, 2009.
- Flesch, T. K., Verge, X. P. C., Desjardins, R. L., and Worth, D.: Methane emissions from a swine manure tank in western Canada, *Canadian Journal of Animal Science*, 93, 159–169, 10.4141/Cjas2012-072, 2013.
- 505 Gao, Z. L., Desjardins, R. L., and Flesch, T. K.: Assessment of the uncertainty of using an inverse dispersion technique to measure methane emissions from animals in a barn and in a small pen, *Atmospheric Environment*, 44, 3128–3134, 10.1016/j.atmosenv.2010.05.032, 2010.
- Gerber, P. J.: Tackling climate change through livestock: A global assessment of emissions and mitigation opportunities, Food and Agriculture Organization of the United Nations FAO, Rome 2013.
- Häni, C., Flechard, C., Neftel, A., Sintermann, J., and Kupper, T.: Accounting for field-scale dry deposition in backward Lagrangian stochastic dispersion modelling of NH₃ emissions, *Atmosphere*, 9, 146, 10.3390/atmos9040146, 2018.
- 510 Hrad, M., Vesenmaier, A., Flandorfer, C., Piringer, M., Stenzel, S., and Huber-Humer, M.: Comparison of forward and backward Lagrangian transport modelling to determine methane emissions from anaerobic digestion facilities, *Atmospheric Environment X*, 12, 100131, ARTN 100131 10.1016/j.aeaoa.2021.100131, 2021.
- Laubach, J., Bai, M., Pinares-Patino, C. S., Phillips, F. A., Naylor, T. A., Molano, G., Rocha, E. A. C., and Griffith, D. W. T.: Accuracy of micrometeorological techniques for detecting a change in methane emissions from a herd of cattle, *Agricultural and Forest Meteorology*, 176, 50–63, 10.1016/j.agrformet.2013.03.006, 2013.
- 515 McGinn, S. M., Flesch, T. K., Harper, L. A., and Beauchemin, K. A.: An approach for measuring methane emissions from whole farms, *J Environ Qual*, 35, 14–20, 10.2134/jeq2005.0250, 2006.
- Sommer, S. G., Christensen, M. L., Schmidt, T., and Jensen, L. S.: Animal manure recycling, John Wiley & Sons, Ltd, Chichester, UK, 10.1002/9781118676677, 2013.
- 520 Stoeker, T. F., Qin, D., Plattner, G. K., Alexander, L. V., Allen, S. K., Bindoff, N. L., F. M., B., Church, J. A., Cubasch, U., Emori, S., Forster, P., P., F., Gillett, N., Gregory, J. M., Hartmann, D. L., Jansen, E., Kirtman, B., Knutti, R., Krishna Kumar, K., Lemke, P., Marotzke, J., Masson-Delmotte, V., Meehl, G. A., Mokhov, I. I., Piao, S., Ramaswamy, V., Randall, D., Rhein, M., Rojas, M., Sabine, C., Shindell, D., Talley, L. D., Vaughan, D. G., and Xie, S. P.: Technical Summary: In: *Climate Change 2013: The Physical Science Basis. Contribution of Working Group I to the Fifth Assessment Report of the Intergovernmental Panel on Climate Change*, 2013.
- 525 VanderZaag, A. C., Gordon, R. J., Glass, V. M., and Jamieson, R. C.: Floating covers to reduce gas emissions from liquid manure storages: A review, *Applied Engineering in Agriculture*, 24, 657–671, 10.13031/2013.25273, 2008.
- Arias, P., Bellouin, N., Coppola, E., Jones, R., Krinner, G., Marotzke, J., Naik, V., Palmer, M., Plattner, G. K., Rogelj, J., 530 Rojas, M., Sillmann, J., Storelvmo, T., Thorne, P., Trewin, B., Rao, K., Adhikary, B., Allan, R., Armour, K., and Ziekfeld, K.: IPCC AR6 WGI Technical Summary, in: 33–144, 10.1017/9781009157896.002, 2021.
- Baldé, H., VanderZaag, A. C., Burt, S., Evans, L., Wagner-Riddle, C., Desjardins, R. L., and MacDonald, J. D.: Measured versus modeled methane emissions from separated liquid dairy manure show large model underestimates, *Agriculture, Ecosystems & Environment*, 230, 261–270, 10.1016/j.agee.2016.06.016, 2016.
- 535 Bühler, M., Häni, C., Ammann, C., Brönnimann, S., and Kupper, T.: Using the inverse dispersion method to determine methane emissions from biogas plants and wastewater treatment plants with complex source configurations, *Atmospheric Environment X*, 13, 100161, 10.1016/j.aeaoa.2022.100161, 2022.
- Bühler, M., Häni, C., Ammann, C., Mohn, J., Neftel, A., Schrade, S., Zähler, M., Zeyer, K., Brönnimann, S., and Kupper, T.: Assessment of the inverse dispersion method for the determination of methane emissions from a dairy housing, *Agricultural and Forest Meteorology*, 307, 108501, 10.1016/j.agrformet.2021.108501, 2021.
- 540 Flesch, T. K., Wilson, J. D., and Harper, L. A.: Deducing ground-to-air emissions from observed trace gas concentrations: A field trial with wind disturbance, *Journal of Applied Meteorology*, 44, 475–484, Doi 10.1175/Jam2214.1, 2005a.
- Flesch, T. K., Wilson, J. D., and Yee, E.: Backward-Time Lagrangian Stochastic Dispersion Models and Their Application to Estimate Gaseous Emissions, *Journal of Applied Meteorology*, 34, 1320–1332, Doi 10.1175/1520-545 (1995)034<1320:Bltsdm>2.0.Co;2, 1995.
- 545

Formatted: References

Formatted: Font: 6 pt

- Flesch, T. K., Wilson, J. D., Harper, L. A., and Crenna, B. P.: Estimating gas emissions from a farm with an inverse dispersion technique, *Atmospheric Environment*, 39, 4863–4874, [10.1016/j.atmosenv.2005.04.032](https://doi.org/10.1016/j.atmosenv.2005.04.032), 2005b.
- Flesch, T. K., Wilson, J. D., Harper, L. A., Crenna, B. P., and Sharpe, R. R.: Deducing ground-to-air emissions from observed trace gas concentrations: A field trial, *Journal of Applied Meteorology*, 43, 487–502, [Doi-10.1175/1520-0450\(2004\)043<0487:Dgefot>2.0.Co;2](https://doi.org/10.1175/1520-0450(2004)043<0487:Dgefot>2.0.Co;2), 2004.
- Gao, Z. L., Desjardins, R. L., and Flesch, T. K.: Assessment of the uncertainty of using an inverse dispersion technique to measure methane emissions from animals in a barn and in a small pen, *Atmospheric Environment*, 44, 3128–3134, [10.1016/j.atmosenv.2010.05.032](https://doi.org/10.1016/j.atmosenv.2010.05.032), 2010.
- Gerber, P. J.: Tackling climate change through livestock: A global assessment of emissions and mitigation opportunities, Food and Agriculture Organization of the United Nations FAO, Rome 2013.
- Häni, C., Bühler, M., Neftel, A., Ammann, C., and Kupper, T.: Performance of open-path GasFinder3 devices for CH₄ and CO₂ concentration measurements close to ambient levels, *Atmospheric Measurement Techniques*, 14, 1733–1741, [10.5194/amt-14-1733-2021](https://doi.org/10.5194/amt-14-1733-2021), 2021.
- Häni, C., Flechard, C., Neftel, A., Sintermann, J., and Kupper, T.: Accounting for Field-Scale Dry Deposition in Backward Lagrangian Stochastic Dispersion Modelling of NH₃ Emissions, *Atmosphere*, 9, 146, [10.3390/atmos9040146](https://doi.org/10.3390/atmos9040146), 2018.
- Harper, L. A., Denmead, O. T., and Flesch, T. K.: Micrometeorological techniques for measurement of enteric greenhouse gas emissions, *Animal Feed Science and Technology*, 166–67, 227–239, [10.1016/j.anifeedsci.2011.04.013](https://doi.org/10.1016/j.anifeedsci.2011.04.013), 2011.
- Hrad, M., Vesenmaier, A., Flandorfer, C., Piringner, M., Stenzel, S., and Huber-Humer, M.: Comparison of forward and backward Lagrangian transport modelling to determine methane emissions from anaerobic digestion facilities, *Atmospheric Environment X*, 12, 100131, [ARTN-100131](https://doi.org/10.1016/j.aeaoa.2021.100131), [10.1016/j.aeaoa.2021.100131](https://doi.org/10.1016/j.aeaoa.2021.100131), 2021.
- Saunio, M., Stavert, A. R., Poulter, B., Bousquet, P., Canadell, J. G., Jackson, R. B., Raymond, P. A., Dlugokencky, E. J., Houweling, S., Patra, P. K., Ciais, P., Arora, V. K., Bastviken, D., Bergamaschi, P., Blake, D. R., Brailsford, G., Bruhwiler, L., Carlson, K. M., Carrol, M., Castaldi, S., Chandra, N., Crevoisier, C., Crill, P. M., Covey, K., Curry, C. L., Etiopie, G., Frankenberg, C., Gedney, N., Hegglin, M. I., Hoglund-Isaksson, L., Hugelius, G., Ishizawa, M., Ito, A., Janssens-Maenhout, G., Jensen, K. M., Joos, F., Kleinen, T., Krummel, P. B., Langenfelds, R. L., Laruelle, G. G., Liu, L. C., Machida, T., Maksyutov, S., McDonald, K. C., McNorton, J., Miller, P. A., Melton, J. R., Morino, I., Müller, J., Murguía-Flores, F., Naik, V., Niwa, Y., Noce, S., Doherty, S. O., Parker, R. J., Peng, C. H., Peng, S. S., Peters, G. P., Prigent, C., Prinn, R., Ramonet, M., Regnier, P., Riley, W. J., Rosentretter, J. A., Segers, A., Simpson, I. J., Shi, H., Smith, S. J., Steele, L. P., Thornton, B. F., Tian, H. Q., Tohjima, Y., Tubiello, F. N., Tsuruta, A., Viovy, N., Voulgarakis, A., Weber, T. S., van Weele, M., van der Werf, G. R., Weiss, R. F., Worthy, D., Wunch, D., Yin, Y., Yoshida, Y., Zhang, W. X., Zhang, Z., Zhao, Y. H., Zheng, B., Zhu, Q., Zhu, Q. A., and Zhuang, Q. L.: The Global Methane Budget 2000–2017, *Earth System Science Data*, 12, 1561–1623, [10.5194/essd-12-1561-2020](https://doi.org/10.5194/essd-12-1561-2020), 2020.
- Sommer, S. G., Christensen, M. L., Schmidt, T., and Jensen, L. S.: *Animal Manure Recycling*, John Wiley & Sons, Ltd, Chichester, UK, [10.1002/9781118676677](https://doi.org/10.1002/9781118676677), 2013.
- Arias, P., Bellouin, N., Coppola, E., Jones, R., Krinner, G., Marotzke, J., Naik, V., Palmer, M., Plattner, G. K., Rogelj, J., Rojas, M., Sillmann, J., Storelvmo, T., Thorne, P., Trewin, B., Rao, K., Adhikary, B., Allan, R., Armour, K., and Ziekfeld, K.: IPCC AR6 WGI Technical Summary, in, 33–144, <https://doi.org/10.1017/9781009157896.002>, 2021.
- Baldé, H., VanderZaag, A. C., Burt, S., Evans, L., Wagner-Riddle, C., Desjardins, R. L., and MacDonald, J. D.: Measured versus modeled methane emissions from separated liquid dairy manure show large model underestimates, *Agriculture, Ecosystems & Environment*, 230, 261–270, <https://doi.org/10.1016/j.agee.2016.06.016>, 2016.
- Bühler, M., Häni, C., Ammann, C., Brönnimann, S., and Kupper, T.: Using the inverse dispersion method to determine methane emissions from biogas plants and wastewater treatment plants with complex source configurations, *Atmospheric Environment X*, 13, 100161, <https://doi.org/10.1016/j.aeaoa.2022.100161>, 2022.
- Bühler, M., Häni, C., Ammann, C., Mohr, J., Neftel, A., Schrade, S., Zähler, M., Zeyer, K., Brönnimann, S., and Kupper, T.: Assessment of the inverse dispersion method for the determination of methane emissions from a dairy housing, *Agricultural and Forest Meteorology*, 307, 108501, <https://doi.org/10.1016/j.agrformet.2021.108501>, 2021.

- 595 Flesch, T. K., Wilson, J. D., and Harper, L. A.: Deducing ground-to-air emissions from observed trace gas concentrations: A field trial with wind disturbance, *Journal of Applied Meteorology*, 44, 475–484, <https://doi.org/10.1175/Jam2214.1.2005a>.
- Flesch, T. K., Wilson, J. D., and Yee, E.: Backward Time Lagrangian Stochastic Dispersion Models and Their Application to Estimate Gaseous Emissions, *Journal of Applied Meteorology*, 34, 1320–1332, [https://doi.org/10.1175/1520-0450\(1995\)034<1320:Bltsdm>2.0.Co;2](https://doi.org/10.1175/1520-0450(1995)034<1320:Bltsdm>2.0.Co;2), 1995.
- 600 Flesch, T. K., Harper, L. A., Powell, J. A., and Wilson, J. D.: Inverse-Dispersion Calculation of Ammonia Emissions from Wisconsin Dairy Farms, *Transactions of the Asabe*, 52, 253–265, <https://doi.org/10.13031/2013.25946>, 2009.
- Flesch, T. K., Wilson, J. D., Harper, L. A., and Crenna, B. P.: Estimating gas emissions from a farm with an inverse-dispersion technique, *Atmospheric Environment*, 39, 4863–4874, <https://doi.org/10.1016/j.atmosenv.2005.04.022>, 2005b.
- 605 Flesch, T. K., Wilson, J. D., Harper, L. A., Crenna, B. P., and Sharpe, R. R.: Deducing ground-to-air emissions from observed trace gas concentrations: A field trial, *Journal of Applied Meteorology*, 43, 487–502, [https://doi.org/10.1175/1520-0450\(2004\)043<0487:Dgefot>2.0.Co;2](https://doi.org/10.1175/1520-0450(2004)043<0487:Dgefot>2.0.Co;2), 2004.
- Gao, Z. L., Desjardins, R. L., and Flesch, T. K.: Assessment of the uncertainty of using an inverse-dispersion technique to measure methane emissions from animals in a barn and in a small pen, *Atmospheric Environment*, 44, 3128–3134, <https://doi.org/10.1016/j.atmosenv.2010.05.032>, 2010.
- 610 Gerber, P. J., Steinfeld, H., Henderson, B. B., Mottet, A., Opio, C. I., Dijkman, J., Faluucci, A., and Tempio, G.: Tackling climate change through livestock—A global assessment of emissions and mitigation opportunities, Food and Agricultural Organization of the United Nations (FAO), Rome, 2013.
- Häni, C., Bühler, M., Neftel, A., Ammann, C., and Kupper, T.: Performance of open-path GasFinder3 devices for CH₄ concentration measurements close to ambient levels, *Atmospheric Measurement Techniques*, 14, 1733–1741, <https://doi.org/10.5194/amt-14-1733-2021>, 2021.
- 615 Häni, C., Flechard, C., Neftel, A., Sintermann, J., and Kupper, T.: Accounting for Field-Scale Dry Deposition in Backward Lagrangian Stochastic Dispersion Modelling of NH₃ Emissions, *Atmosphere*, 9, 146, <https://doi.org/10.3390/atmos9040146>, 2018.
- Häni, C., Neftel, A., Flechard, C., Amman, C., Valach, A., and Kupper, T.: Validation of a short-range dispersion and deposition model using field-scale ammonia and methane release experiments, *Agricultural and Forest Meteorology*, submitted.
- 620 Harper, L. A., Denmead, O. T., and Flesch, T. K.: Micrometeorological techniques for measurement of enteric greenhouse gas emissions, *Animal Feed Science and Technology*, 166–67, 227–239, <https://doi.org/10.1016/j.anifeedsci.2011.04.013>, 2011.
- 625 Hrad, M., Vesenmaier, A., Flandorfer, C., Piringner, M., Stenzel, S., and Huber-Humer, M.: Comparison of forward and backward Lagrangian transport modelling to determine methane emissions from anaerobic digestion facilities, *Atmospheric Environment X*, 12, 100131, <https://doi.org/10.1016/j.aeaoa.2021.100131>, 2021.
- Laubach, J., Bai, M., Pinares-Patino, C. S., Phillips, F. A., Naylor, T. A., Molano, G., Rocha, E. A. C., and Griffith, D. W. T.: Accuracy of micrometeorological techniques for detecting a change in methane emissions from a herd of cattle, *Agricultural and Forest Meteorology*, 176, 50–63, <https://doi.org/10.1016/j.agrformet.2013.03.006>, 2013.
- 630 McGinn, S. M., Flesch, T. K., Harper, L. A., and Beauchemin, K. A.: An approach for measuring methane emissions from whole farms, *J Environ Qual*, 35, 14–20, <https://doi.org/10.2134/jeq2005.0250>, 2006.
- Saunio, M., Stavert, A. R., Poulter, B., Bousquet, P., Canadell, J. G., Jackson, R. B., Raymond, P. A., Dlugokencky, E. J., Houweling, S., Patra, P. K., Ciais, P., Arora, V. K., Bastviken, D., Bergamaschi, P., Blake, D. R., Brailsford, G., Bruhwiler, L., Carlson, K. M., Carrol, M., Castaldi, S., Chandra, N., Crevoisier, C., Crill, P. M., Covey, K., Curry, C. L., Etiope, G., Frankenberg, C., Gedney, N., Hegglin, M. I., Hoglund-Isaksson, L., Hugelius, G., Ishizawa, M., Ito, A., Janssens-Maenhout, G., Jensen, K. M., Joos, F., Kleinen, T., Krummel, P. B., Langenfelds, R. L., Laruelle, G. G., Liu, L. C., Machida, T., Maksyutov, S., McDonald, K. C., McNorton, J., Miller, P. A., Melton, J. R., Morino, I., Müller, J., Murguía-Flores, F., Naik, V., Niwa, Y., Noce, S., Doherty, S. O., Parker, R. J., Peng, C. H., Peng, S. S., Peters, G. P., Prigent, C., Prinn, R., Ramonet, M., Regnier, P., Riley, W. J., Rosentreter, J. A., Segers, A., Simpson, I. J., Shi, H., Smith, S. J., Steele, L. P., Thornton, B. F., Tian, H. Q., Tohjima, Y., Tubiello, F. N., Tsuruta, A., Viovy, N., Voulgarakis, A., Weber, T. S., van Weele, M., van der Werf, G. R., Weiss, R. F., Worthy, D., Wunch, D., Yin, Y., Yoshida, Y., Zhang, W. X., Zhang, Z., Zhao, Y. H., Zheng, B., Zhu, Q., Zhu, Q. A., and Zhuang, Q. L.: The Global Methane Budget 2000–2017, *Earth System Science Data*, 12, 1561–1623, <https://doi.org/10.5194/essd-12-1561-2020>, 2020.

645 Sommer, S. G., Christensen, M. L., Schmidt, T., and Jensen, L. S.: Animal Manure Recycling, John Wiley & Sons, Ltd,
Chichester, UK, <https://doi.org/10.1002/9781118676677>, 2013.
VanderZaag, A. C., Flesch, T. K., Desjardins, R. L., Balde, H., and Wright, T.: Measuring methane emissions from two dairy
farms: Seasonal and manure management effects, *Agricultural and Forest Meteorology*, 194, 259-267,
650 <https://doi.org/10.1016/j.agrformet.2014.02.003>, 2014.